

HiSST: 4th International Conference on High-Speed Vehicle Science & Technology



22–26 September 2025, Tours, France

Investigation of spallation and volumetric ablation products in TPS materials during plasma facility experiments

Kate B. Rhoads ¹ Kristen J. Price¹, Stefan Loehle², Savio J. Poovathingal¹, Alexandre Martin¹

Abstract

Ablative thermal protection systems (TPS) are used during atmospheric entry to mitigate thermal energy transport to the substructure of spacecraft through material degradation. In order to better understand in-depth material changes due to volumetric ablation, previously tested samples were re-exposed to a pure oxygen environment in the High Enthalpy Low-Cost Multi-Use Torch (HELMUT) facility at the University of Kentucky. Additionally, PICA samples were tested to investigate the impact phenolic resin has on the material response. Scanning electron microscopy (SEM) was conducted on disconnected fibers that remained on the samples after flow exposure to investigate in-depth fiber and binder pitting. Material response across test campaigns was compared to evaluate changes in structural integrity caused by in-depth oxidation, which is suspected to affect spallation behavior. Re-exposure produced higher percent volume loss, greater percent mass loss, and a reduction in density. PICA samples produced a negligible fiber layer, and a lower percent volume loss. These findings indicate that FiberForm tested in the HELMUT facility could be operating in a reaction-limited regime, with substantial oxygen penetration beneath the surface. This methodology also establishes a framework for providing degree of char estimates for material response models, and highlights the role phenolic resin has on structural integrity.

Keywords: volumetric ablation, spallation, in-depth oxidation

Nomenclature

Latin

m - Mass [g]

V – Volume [mm 3]

Greek

 ρ – Density [g/mm³]

Subscripts

t - Total (sample + holder)

h - Holder

 $0\,$ – Initial/original state

u – Unexposed portion

e – Exposed portion

1. Introduction

Spacecraft used for atmospheric entry are equipped with thermal protection systems (TPS) to prevent substructure heating as kinetic energy gets converted to thermal energy during deceleration [1–3]. Ablative TPS materials absorb this thermal energy by material removal through mechanisms such as nitridation, oxidation, and sublimation [4,5]. Oxidation is a major contributor to mass loss in TPS materials under both air and CO_2 environments and is also strongly linked to spallation, where particles detach from the bulk material and are transported into the flow [6–9]. Limited information exists regarding mass loss contributions due to spallation, creating a knowledge gap between material response models and flight behavior [10].

Phenolic Impregnated Carbon Ablators (PICA) have been used as TPS during atmospheric entry in heat flux conditions up to $\approx 1000 \, \text{W/cm}^2$ [11,12]. The substrate for this material is a carbon fiber

¹University of Kentucky, Department of Mechanical and Aerospace Engineering, kate.rhoads@uky.edu, saviopoovathingal@uky.edu, alexandre.martin@uky.edu

²University of Stuttgart, High Enthalpy Flow Diagnostics Group, loehle@irs.uni-stuttgart.de

preform known as FiberForm®. This material is produced by forming a porous network of carbon fibers bonded with an organic binder. The assembly is then heat-treated to high temperatures (≈ 2000 °C) to carbonize the binder [13]. The resulting material is an orthotropic carbon fiber matrix in which the fibers are bonded by a carbonized binder. A micro-tomography rendering of FiberForm® can be seen in Fig. 1.

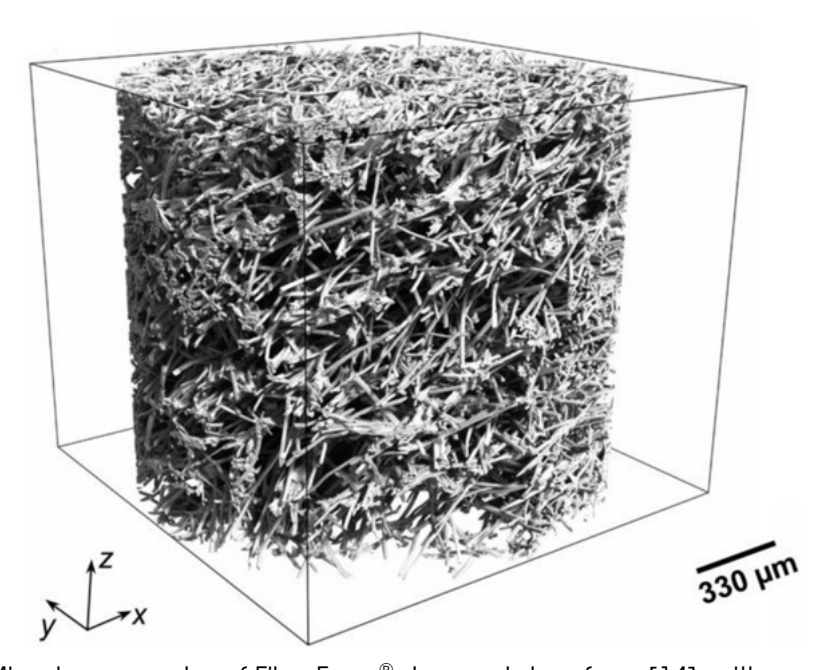


Fig 1. Microtomography of FiberForm®. Image taken from [14], with permission.

Volumetric ablation refers to in-depth changes to the bulk TPS during flow exposure [15,16]. This phenomenon can occur through fiber pitting and binder oxidation, leading to pore growth, increased permeability, and reduced structural integrity. In particular, if the binder ablates at a faster rate than the carbon fibers, weakened connections may form, allowing for additional mass loss through mechanical processes such as spallation [5]. Observed spallation in the High Enthalpy Low-cost Multi-Use Torch (HELMUT) at the University of Kentucky is shown in Fig 2. While experimental data exist on the response of FiberForm® in oxygen-rich environments, the associated in-depth structural evolution remains less well understood.

2. Background

2.1. Facility Overview

A plasma facility known as the High Enthalpy Low-cost Multi-Use Torch (HELMUT) exists at the University of Kentucky and is capable of simulating flight-relevant heating and pressure conditions during atmospheric entry [18]. This facility became re-operational in February 2024 and offers a cost-effective means of testing TPS materials and can operate without the use of shielding gases. As a result, this electrode-less facility allows for samples to be exposed directly to highly reactive environments, including partially dissociated oxygen relevant to flight environments. [19]. These capabilities allow for the investigation of the oxidation contributions to mass loss. Fig 3 shows an image of the test facility and Table 1 provides details on the specifications.

Another distinguishing characteristic of HELMUT is the orientation of the test article. Plasma is generated at the top of the chamber and directed downward, such that the exposed ablative surface of the sample is oriented upward. This configuration can be seen in Fig 2. When running in low-velocity flow conditions, the presence of shear is minimal, which has shown to result in quantities of in-depth ablation products remaining on the sample surface of FiberForm® after testing. Previous work has been completed regarding the in-depth oxidation contributions to

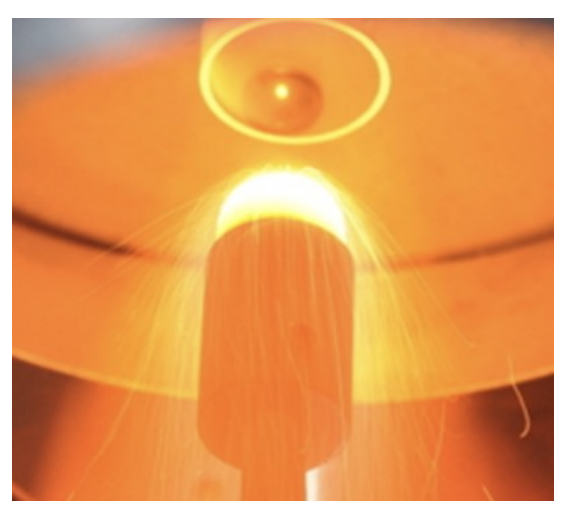


Fig 2. Spallation shown on a FiberForm® sample in the HELMUT facility. Image taken from [17], with permission.

ParameterDescriptionMicrowave Generator Powerup to 3 kWOperating Frequency2.45 GHz

0.1-1 atm

Oxygen, Nitrogen, Air, Argon, Methane

Table 1. HELMUT Facility Specifications

spallation from the presence of this fiber layer [5], but the impacts on ablation rates and material properties have not been conducted. An image of the detached Fibers seen in FiberForm® samples is shown in Fig 4. This image also provides evidence for significant amounts of oxygen flowing through the pores of FiberForm®.

2.2. Previous Experiments

Pressure Range Test Gases

In-depth oxidation experiments conducted in October 2024 revealed that approximately 24% of the total volume loss and 3.5% of the total mass loss observed during pure oxygen testing can be attributed to the previously discussed layer of detached fibers that remained on the sample surface after flow exposure [5]. In each of the nine samples tested, this layer of detached fibers was present. The run conditions for these experiments can be seen in Table 2.

Table 2. HELMUT Facility Run Conditions

Parameter	Description
Microwave Generator Power	1.5 kW
Operating Frequency	2.45 GHz
Pressure Tested	0.1 atm
Heat Flux	\sim 30 W/cm 2
Test Gas	Oxygen, 20 slpm

The in-depth material changes observed in the first campaign motivated a second round of testing on the same samples to quantify how reduced density impacts degradation rates. Interest in the role of the phenolic resin on volumetric ablation motivated testing of PICA samples



Fig 3. HELMUT Facility Overview.

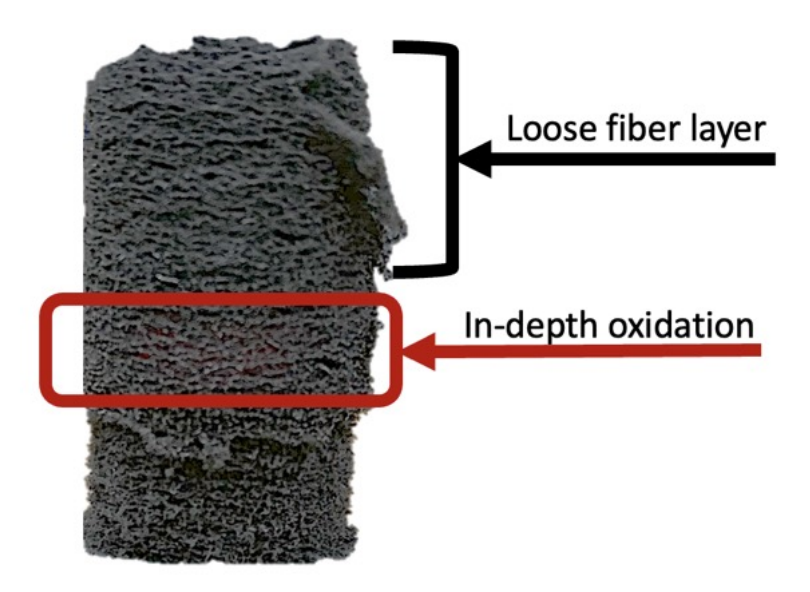


Fig 4. Oxidation occurring in-depth in a FiberForm sample. It can be seen that there is a region of loose detached fibers potentially caused by oxygen remaining in the sample post-test.

under the same conditions. A better understanding of bulk material behavior in oxygen-rich environments could provide critical insight in distinguishing oxidation regimes, characterizing char layer development, and improving the accuracy of TPS material response models.

3. Experimental Description

Thus, an experimental campaign was carried out in the HELMUT facility using previously tested FiberForm samples and virgin PICA samples with the goal of assessing how volumetric ablation influences material behavior during testing. For this campaign, four samples from the October 2024 campaign were chosen to be re-exposed to the same conditions described in Table 2, and two PICA samples were exposed to the same conditions. Pre-test images of the four FiberForm samples tested can be seen in Figure 5, and the original geometry prior to the previous campaign is shown in Fig 6. The sample names correspond to the sample ID from the previously conducted experiments. Figure 7 shows the two PICA samples prior to exposure to the plasma flow.



Fig 5. Pre-test images of the samples chosen for re-exposure to the plasma flow.

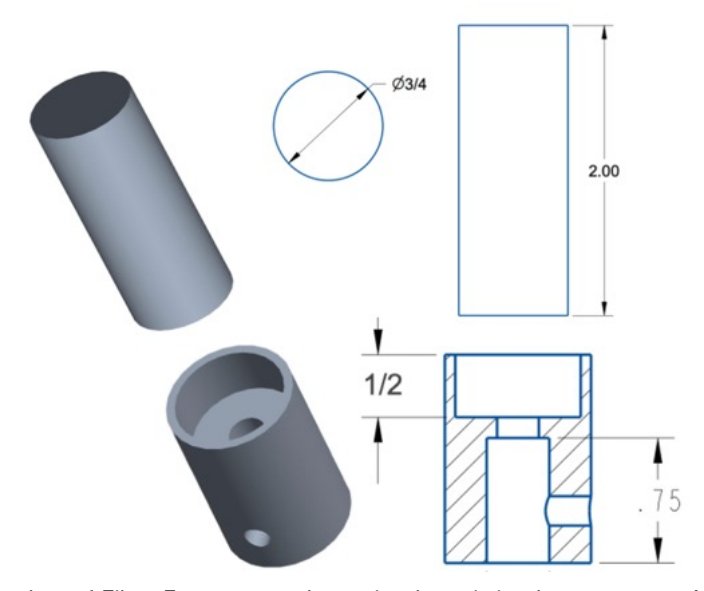


Fig 6. Original geometry of FiberForm samples prior to original exposure. All dimensions are in inches. Image taken from [5], with permission.

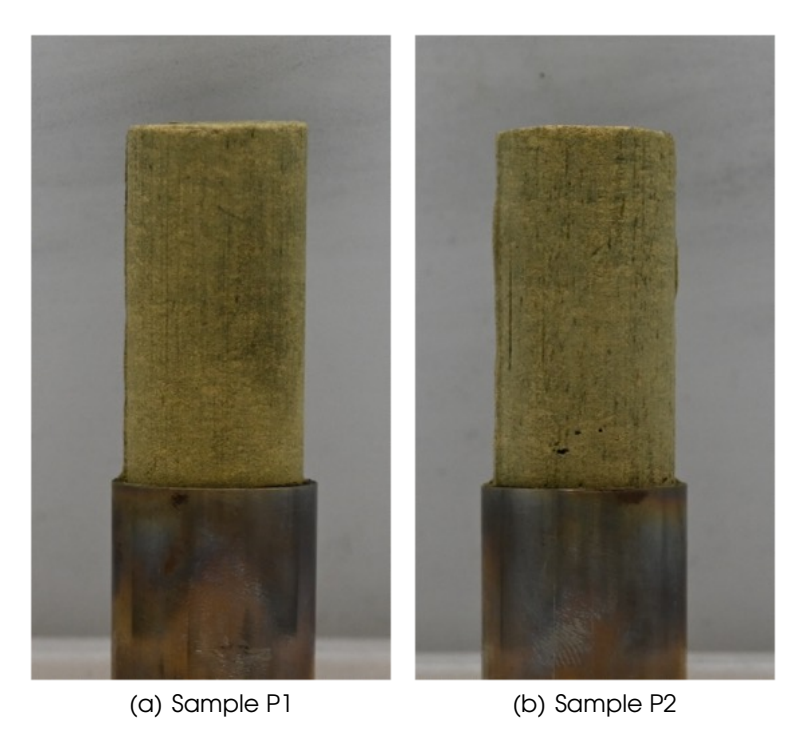


Fig 7. Pre-test images of the PICA samples exposed to the plasma flow.

4. Results

4.1. Observation of in-depth oxidation

Upon sample removal, it was observed that the interior regions of the FiberForm samples remained visibly glowing. This sustained glow provides clear evidence that oxygen was able to penetrate beneath the outer surface and participate in reactions within the interior of the material. An image of this phenomenon seen in sample 1R is shown in Fig. 8. This observed process further highlights the presence and significance of volumetric ablation in oxygen-rich environments.

4.2. Volume loss results

Using the same methodology as in previous experiments, volume loss values for the tested samples were obtained with a 3D scanner. Measurements were performed both with and without the fiber layer present for the FiberForm samples in order to estimate the contribution of spallation to the overall volume loss in these experiments. In addition, overlay images were generated to provide a visual representation of the significance of the intact fiber layers remaining on the sample surfaces after exposure. Fig. 9 presents the overlay images of the tested samples, while Table 3 summarizes the corresponding volume loss results.

It is suspected that the phenolic resin increased the structural integrity of the PICA material, preventing samples P1 and P2 from exhibiting this fiber layer. Post-test images of these samples are shown in Fig.10, and the corresponding volume loss results are also listed in Table 3. Once the phenolic resin fully pyrolizes, the remaining FiberForm substrate is expected to define the char layer. Volumetric ablation results from FiberForm under the same conditions provide critical insight into the behavior of PICA after resin pyrolysis and can improve material response model predictions of char layer recession.

To compare the bulk material behavior between the 2024 experiments and the subsequent retests, the percent total exposed volume loss was calculated for each run using the original and final volumes of the four re-exposed samples. The results show that a greater fraction of bulk



Fig 8. In-depth oxidation of FiberForm prior to sample removal from the flow.

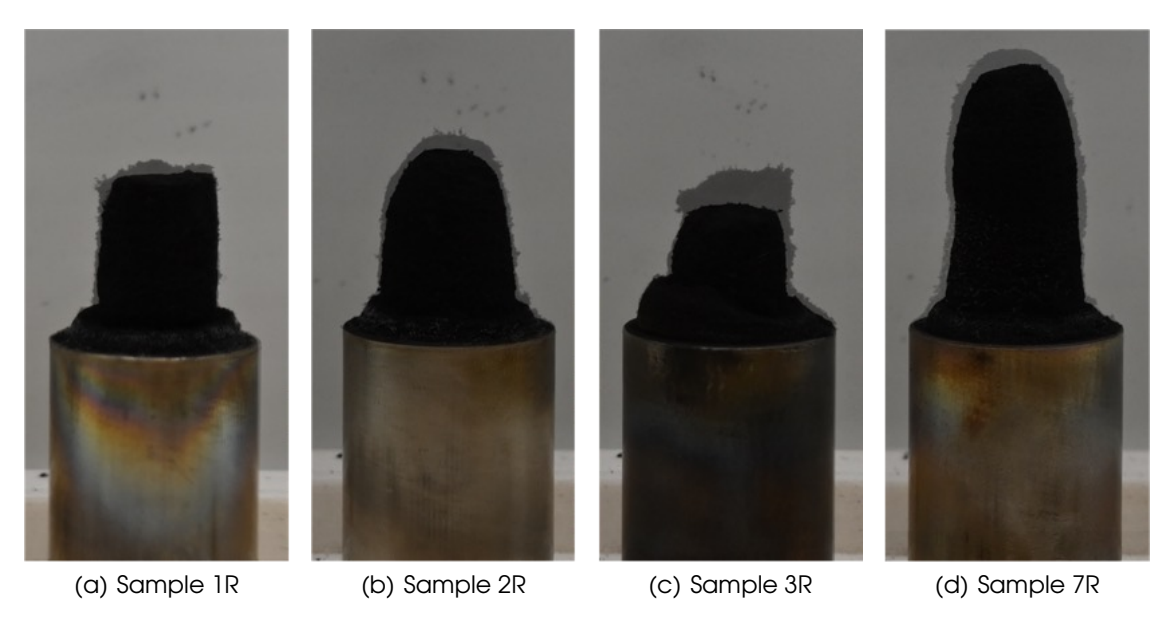


Fig 9. Post-test images of the samples chosen for re-exposure to the plasma flow. These figures highlight the profiles of the loose fibers remaining on the sample surfaces after testing.

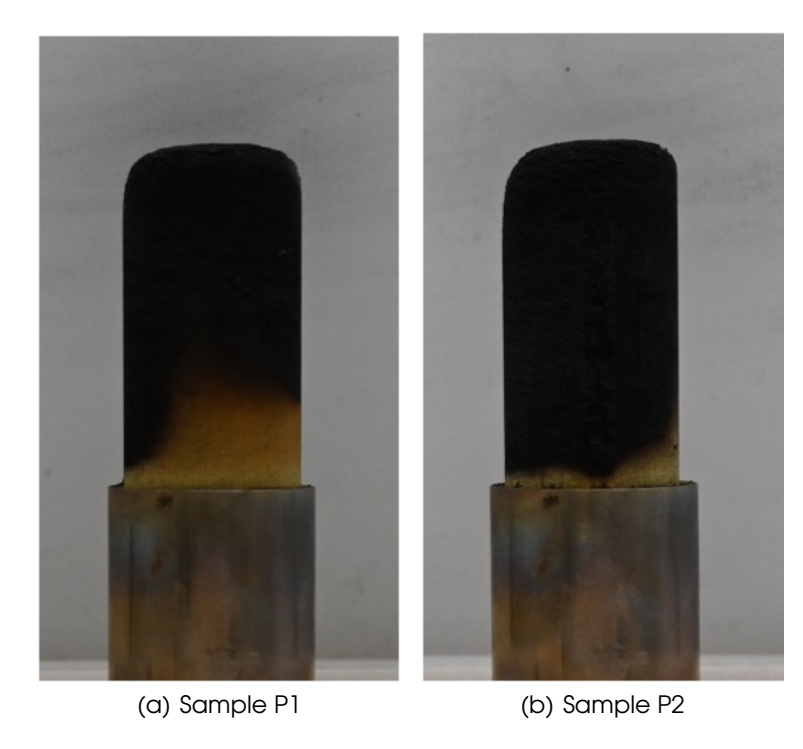


Fig 10. Post-test images of the PICA samples exposed to the plasma flow. These figures highlight the increased structural integrity due to the phenolic resin.

Table 3. Sample exposed volume data for each run

Run Number	Original Volume (mm ³)	Fiber Layer Volume (mm ³)	Final Volume (mm³)
1R	7966	2447	1939
2R	5285	2563	2279
3R	5872	2086	1575
7R	6349	3740	3403
P1	10859	N/A	9504
P2	11004	N/A	9161

volume was lost during the re-tests. These results are consistent with expected behavior of enhanced oxidation from the reduction in density during the first exposure. These results are summarized in Table 4. On average, the re-tested samples exhibited a volume loss of approximately 40% during the first run and 63% during the second run, corresponding to an increase of about 58% when re-exposed to the same conditions. The PICA samples exhibited approximately 14.6% volume loss with exposure to the same conditions, resulting from the additional phenolic resin in the material. This observation further supports the hypothesis that in-depth oxidation influences material behavior. The phenolic resin in PICA may also inhibit oxygen transport, contributing to the reduced volume loss observed.

4.3. Mass loss results

For comparison with the previous experiments, the total mass loss was measured and recorded for each run, both with and without the loose layer of detached fibers remaining after testing. The results for all of the tested samples are provided in Table 5. On average, the re-tested samples exhibited a total mass loss of approximately 0.7 g per test, highlighting the continued degradation of material when subjected to re-exposure. The average mass loss due to the fiber

Table 4. Percent total volume loss between first and second exposure

Run Number	Percent loss during first exposure	Percent loss during second exposure
1R	27.3%	75.7%
2R	51.3%	56.9%
3R	44.0%	73.2%
7R	38.5%	46.4%
P1	12.5%	N/A
P2	16.7%	N/A

layer was calculated to be approximately 0.02 g per test. Although there was no fiber layer present, PICA samples exhibited greater mass losses, averaging around 1.63 g per test.

Table 5. Sample mass data including the holder for each run

Run Number	Original mass (g)	Fiber Layer Mass (g)	Final Mass (g)
1R	67.512	66.655	66.643
2R	67.232	66.714	66.701
3R	67.278	66.519	66.499
7R	67.428	66.828	66.804
P1	70.823	N/A	69.097
P2	70.570	N/A	69.043

After subtracting the holder mass, the percent change in mass was also calculated for each of the tested samples and compared with the original mass loss values from the earlier campaign. These results are summarized in Table 6. The analysis shows an average percent mass loss of 34% for FiberForm during the first series of tests and 42% during the second series, corresponding to an increase of roughly 24% between runs. This trend suggests that the reduction in density following the first exposure may enhance oxygen transport into the bulk material. The mass loss percentage was approximately 33% for the PICA samples, which is similar to the mass loss rates of the FiberForm after first exposure. An increase in porosity and permeability after the first FiberForm tests could result in the accelerated mass loss during re-testing. These results provide preliminary evidence that the oxygen atoms in the HELMUT facility could be reaction limited rather than diffusion limited when interacting with FiberForm at these conditions, as there is significant transport of oxygen into the material. [20].

Table 6. Percent total mass loss between first and second exposure excluding the steel holder

Run Number	Percent loss during first exposure	Percent loss during second exposure
1R	28.5%	48.4%
2R	41.3%	35.1%
3R	36.7%	49.9%
7R	30.1%	36.5%
P1	35.1%	N/A
P2	31.5%	N/A

4.4. In-depth ablation analysis

4.4.1. Bulk density

In order to estimate the amount of volumetric ablation that occurred in the samples, it was of interest to estimate the density of the exposed FiberForm after testing. The methodology of obtaining the density after the first exposure is discussed in this section. The holder mass, m_h , is first subtracted from the measured total mass of the sample and holder assembly, m_t ,

$$m_0 = m_t - m_h, \tag{1}$$

to isolate the true mass of the material. The original density of the untested material is then defined as

$$\rho_0 = \frac{m_0}{V_0},\tag{2}$$

where V_0 is the initial volume of the material.

It is assumed that the unexposed portion of the material maintains this original density, ρ_0 . Using the measured unexposed volume inside the holder, V_u , the corresponding unexposed mass is calculated as

$$m_u = \rho_0 V_u. (3)$$

The mass of the exposed portion of the material is then obtained by subtracting the unexposed mass, m_u , from the material mass m_0 using

$$m_e = m_0 - m_u. (4)$$

Finally, the density of the exposed portion is determined by dividing the exposed mass by the measured exposed volume, V_e , from the 3D scans using

$$\rho_e = \frac{m_e}{V_e}. ag{5}$$

This methodology ensures that the contribution of the sample holder is removed from the analysis, and that the density of the exposed region is evaluated independently of both the holder and the unexposed portion.

To obtain the final mass of the exposed FiberForm, the four re-tested samples were cut at the holder tip and weighed. The corresponding 3D scan volume measurements were then used to determine the final density of the material following the second exposure. Density results from these calculations can be seen in table 7.

Table 7. Sample exposed density data for each run

er Original Density (kg/m³) First exposure (kg/m³) Seco

Run Number	Original Density (kg/m³)	First exposure (kg/m³)	Second exposure (kg/m³)
1R	177.9	151.9	109.8
2R	174.6	161.0	139.5
3R	176.1	159.2	120.0
7R	180.5	171.7	140.7
Pl	352.5	221.2	N/A
P2	335.0	230.5	N/A

A significant reduction in bulk density was observed across all of the runs after each exposure to the pure oxygen environment. The percent change in density for each run is reported in Table 8. On average, the first FiberForm cycle produced a reduction of approximately 9.2%, while the second cycle resulted in an average reduction of 21.0%. These results provide further evidence that oxygen quickly penetrates the material microstructure under these conditions, leading to progressive internal material loss. In addition to confirming the role of in-depth oxidation, the density reductions suggest that the initial exposure weakened the microstructure, allowing oxygen to diffuse more effectively into the bulk material during subsequent exposures.

Compared to FiberForm, the PICA samples showed a greater average percent density loss (approximately 34.2%), which is attributed to the low pyrolysis temperatures of the phenolic resin and its influence on significant mass loss with limited volume loss. The density calculation methodology presented in this study can also be used to better understand the remaining char layer. Degree of char in PICA is often estimated by visual inspection of color changes, but combining 3D scanning with mass measurements has the potential to provide a more reliable measure of char formation by quantifying the residual phenolic resin in each layer.

Run Number	Percent loss during first exposure	Percent loss during second exposure
1R	14.6%	27.7%
2R	7.7%	13.4%
3R	9.5%	24.6%
7R	4.9%	18.1%
P1	31.2%	N/A
P2	37.2%	N/A

Table 8. Percent total density loss between first and second exposure

4.4.2. SEM oxidation analysis

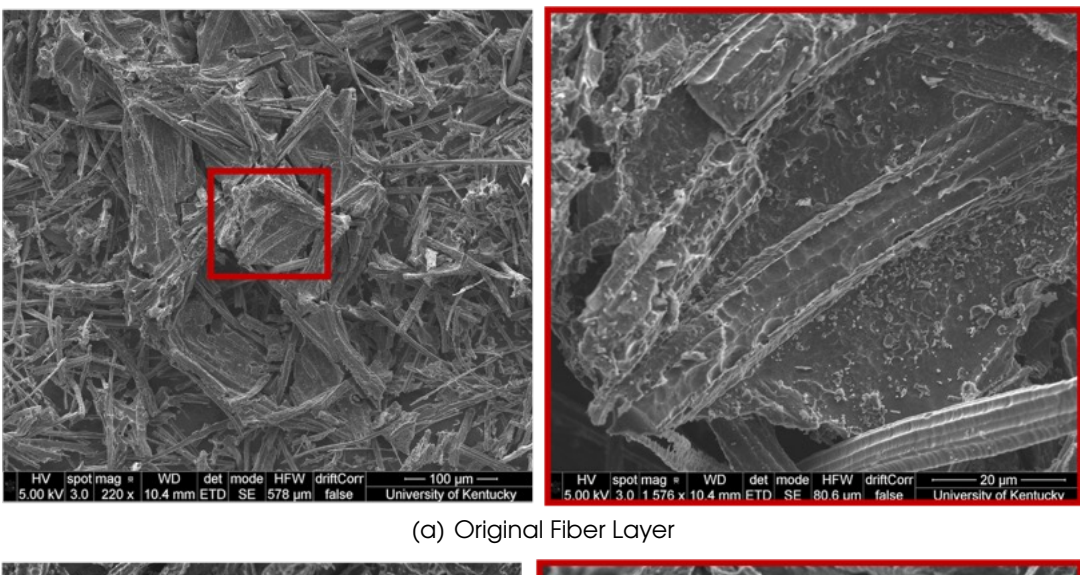
To investigate the presence of preferential binder oxidation, scanning electron microscopy (SEM) was performed on the detached fiber layers to examine microstructural behavior. Representative SEM images are provided in Fig. 11. These images show the fiber layer both following the original test and after re-exposure to the flow. Clear differences in surface morphology are evident between the two conditions. In particular, the re-exposed fibers exhibit a significant increase in both fiber and binder pitting compared to those from the first exposure.

This progression of oxidation is consistent with the measured decrease in bulk density from the previous section. This evidence suggests that oxidation during the first run not only reduced overall material density but also altered the microstructure in a way that allowed for deeper oxygen penetration during re-testing. This progression could result in continuous weakening of fiber connections, resulting in lower structural integrity and a larger potential for spallation. This pitting phenomenon will result in an increase in porosity at the fiber surfaces, which could allow for oxygen transport into the bulk material to happen at a faster rate. These findings indicate that binder oxidation plays a critical role in the overall structural integrity of FiberForm.

5. Conclusions

The re-testing of samples from a previous campaign in pure oxygen revealed that repeated exposure resulted in greater percent volume loss, percent mass loss and reduction in density. SEM results showed further weakening of the carbon binder material. These trends demonstrate that material degradation is not only surface-driven but also increases in-depth with increased exposure time. The results provide evidence for enhanced oxygen transport into the bulk material upon re-exposure through the progressive increase in permeability as these reactions are occurring.

These findings highlight the importance of volumetric ablation in distinguishing between diffusion-



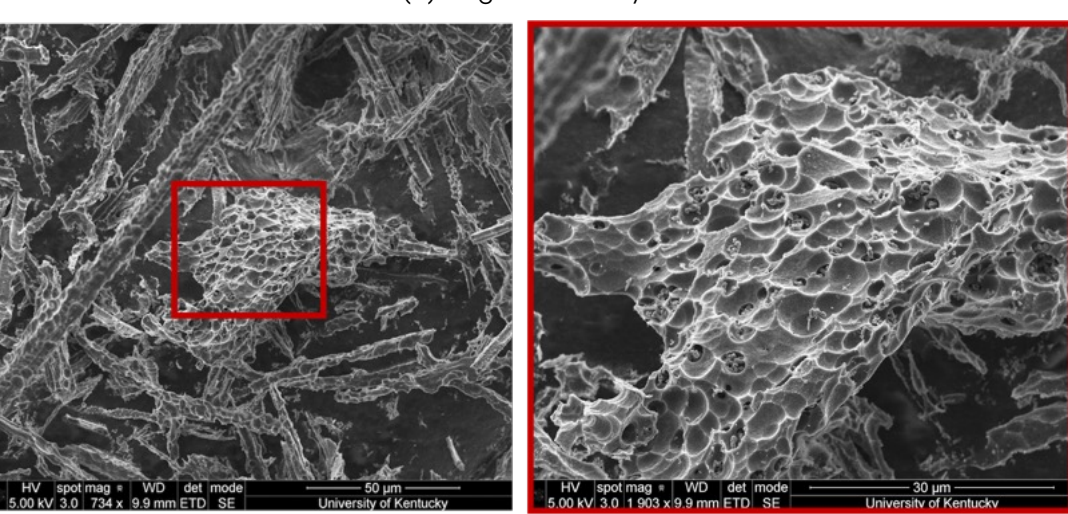


Fig 11. Scanning electron microscopy (SEM) images of the fiber layers captured during HELMUT tests. The original fiber layer from the previous campaign (a), shows less severe binder and fiber pitting compared to the re-exposed tests (b).

(b) Fiber Layer after Re-exposure

limited and reaction-limited oxidation regimes. The substantial in-depth oxygen transport observed in the re-tested samples points toward reaction-limited behavior, as the oxidizing species penetrate the porous material and drive ablation beneath the exposed surface. Recognizing this regime dependence is critical for both improving the accuracy of material response models, and for guiding the design of thermal protection systems in oxygen-rich environments.

Testing PICA under the same oxygen-rich conditions provides a direct comparison for evaluating the influence of the phenolic resin. The resin was shown to aid in maintaining the structure of the carbon fiber matrix during exposure, reducing the extent of the volume loss observed in FiberForm alone. The presence of phenolic resin could also be reducing the oxygen transport, maintaining the FiberForm substrate during the PICA tests. This phenomenon was observed despite the low-velocity, partially dissociated oxygen conditions tested. Evaluating PICA and FiberForm under identical conditions can also provide a clearer understanding of char layer behavior. This direct comparison shows that the resin does more than slow surface recession,

but plays a role in preserving the structural integrity of the bulk thermal protection system. Additionally, the framework for obtaining density values can be used to provide degree of char data that is not based on visual analysis alone, but on remaining phenolic resin in each layer.

6. Acknowledgments

This research was sponsored by the NASA Space Technology Graduate Research Opportunities (NSTGRO) Grant Number 80NSSC24K1348. The authors extend their gratitude to Floyd Taylor and Herb Mefford for their assistance in machining the samples and holders used in this test campaign. Special thanks are also due to Fred Shireman and Shreya Pokharel for their expertise with the SEM machine. Additional thanks to Berk Gur and Dr. Dan Fries for their assistance with sample testing.

pyrolysis is preventing oxygen transport even in low velocity and partially dissociated oxygen environments

References

- [1] F. S. Milos and Y.-K. Chen, "Ablation, thermal response, and chemistry program for analysis of thermal protection systems," *Journal of Spacecraft and Rockets*, vol. 50, no. 1, pp. 137–149, doi:10.2514/1.A32302, 2013.
- [2] R. S. Davuluri, H. Zhang, and A. Martin, "Numerical study of spallation phenomenon in an arc-jet environment," *Journal of Thermophysics and Heat Transfer*, vol. 30, no. 1, pp. 32–41, 2016, doi:10.2514/1.T4586.
- [3] R. Davuluri, S. C. Bailey, K. Tagavi, and A. Martin, "Numerical reconstruction of spalled particle trajectories in an arc-jet environment," in *AIAA SciTech 2021 Forum*, AIAA 2021-1172, (Virtual), January 2021, doi: 10.2514/6.2023-2714.
- [4] J. D. Anderson, Hypersonic and High Temperature Gas Dynamics. AIAA, 1989.
- [5] K. B. Rhoads, K. J. Price, I. M. Wadsworth, S. Loehle, S. J. Poovathingal, and A. Martin, "Evidence of spallation due to volumetric ablation," in AIAA SCITECH 2025 Forum, p. 1425, 2025, doi: 10.2514/6.2025-1425.
- [6] S. C. Bailey, D. Bauer, F. Panerai, S. C. Splinter, P. M. Danehy, J. M. Hardy, and A. Martin, "Experimental analysis of spallation particle trajectories in an arc-jet environment," Experimental Thermal and Fluid Science, vol. 93, pp. 319–325, 2018, doi:10.1016/j.ex-pthermflusci.2018.01.005.
- [7] K. J. Price, R. Davuluri, G. Palmer, S. Bailey, and A. Martin, "Modeling of spalled particles for arc-jet test planning," in *AIAA Aviation 2022 Forum*, p. 3948, 2022, doi:10.2514/6.2022-3948.
- [8] K. J. Price, J. M. Hardy, C. G. Borchetta, F. Panerai, S. C. Bailey, and A. Martin, "Spallation particle size analysis resulting from arc-jet experiments," in *AIAA Aviation 2020 Forum*, AIAA 2020-3279, (Virtual), June 2020, doi: 10.2514/6.2020-3279.
- [9] K. J. Price, S. Bailey, and A. Martin, "Analysis of arc-jet sample spallation products," in *AIAA SCITECH 2024 Forum*, p. 1480, 2024, doi: 10.2514/6.2024-1480.
- [10] R. S. C. Davuluri, H. Zhang, and A. Martin, "Numerical study of spallation phenomenon in an arc-jet environment," *Journal of Thermophysics and Heat Transfer*, vol. 30, no. 1, pp. 32–41, 2016.
- [11] C. Park, "Calculation of stagnation-point heating rates associated with stardust vehicle," *Journal of Spacecraft and Rockets*, vol. 44, pp. 24–32, January–February 2005, doi:10.2514/1.15745.

- [12] H. Weng and A. Martin, "Numerical investigation of thermal response using orthotropic charring ablative material," *Journal of Thermophysics and Heat Transfer*, vol. 29, pp. 429–438, Jul. 2015, doi: 10.2514/1.T4576.
- [13] P. Agrawal, J. F. Chavez-Garcia, and J. Pham, "Fracture in phenolic impregnated carbon ablator," *Journal of Spacecraft and Rockets*, vol. 50, no. 4, pp. 735–741, 2013, doi:10.2514/1.A32389.
- [14] F. Panerai, J. Ferguson, J. Lachaud, A. Martin, M. J. Gasch, and N. N. Mansour, "Analysis of fibrous felts for flexible ablators using synchrotron hard x-ray micro-tomography," in *European Symposium on Aerothermodynamics for Space Vehicles*, no. ARC-E-DAA-TN21716, 2015, doi: 10.13140/RG.2.1.2661.0084.
- [15] J. Lachaud, I. Cozmuta, and N. N. Mansour, "Multiscale approach to ablation modeling of phenolic impregnated carbon ablators," *Journal of Spacecraft and Rockets*, vol. 47, no. 6, pp. 910–921, doi:10.2514/1,42681, 2010.
- [16] E. M. Liston, "Arc-image testing of ablation materials," *Journal of Macromolecular Science—Chemistry*, vol. 3, no. 4, pp. 705–733, 1969, doi: 10.1080/10601326908053837.
- [17] K. Price, "Characterization of the spallation phenomenon in ablative thermal protection system materials resulting from arc-jet experiments," 2024.
- [18] M. Winter and H. Koch, "Low power plasma facilities for the investigation of gas-surface interaction at the university of kentucky," in *53rd AIAA Aerospace Sciences Meeting*, p. 2016, 2015, doi: 10.2514/6.2015-2016.
- [19] H. Koch, B. Butler, M. Winter, and C. Arnold, "Operational envelope of the low power plasma facilities at the university of kentucky," in *46th AIAA Thermophysics Conference*, p. 4152, 2016, doi: 10.2514/6.2016-4152.
- [20] B. M. Ringel, F. Semeraro, J. C. Ferguson, H. S. Barnard, B. Dias, C. M. Schlepütz, E. S. Barnard, S. Schickler, K. Levy, S. Shacterman, T. Benioff-White, J. Davis, A. A. MacDowell, D. Y. Parkinson, and F. Panerai, "Carbon fiber oxidation in 4D," *Advanced Materials*, 2025, 10.1002/adma.202502007.